

Solution-Processed Molecular Bis(Naphthalene Diimide) Derivatives with High Electron Mobility

Lauren E. Polander,^{†,§} Shree P. Tiwari,^{‡,§,||} Laxman Pandey,^{†,§} Brian M. Seifried,^{†,§} Qing Zhang,^{†,§} Stephen Barlow,^{†,§} Chad Risko,^{†,§} Jean-Luc Brédas,^{†,§} Bernard Kippelen,^{*,†,§} and Seth R. Marder^{*,†,§}[†]School of Chemistry and Biochemistry, [‡]School of Electrical and Computer Engineering, and [§]Center for Organic Photonics and Electronics, Georgia Institute of Technology, Atlanta, Georgia 30332-0400, United States

Supporting Information

KEYWORDS: electronic materials, organic semiconductors, naphthalene diimide

Organic semiconductors have attracted interest for electronic applications because of their potential for use in low-cost, large-area, flexible electronic devices.^{1–3} While many examples of organic semiconductors for p-channel and n-channel organic field-effect transistors (OFETs) have been reported in the recent literature,^{4–6} there is a paucity of high-performance, solution-processable, small-molecule materials for n-channel OFETs. In order to take advantage of the technological potential of organic semiconducting materials, solution-processable, ideally air-stable, electron-transport (ET) materials with low barriers for charge injection, high charge-carrier mobility values ($>1 \text{ cm}^2 \text{ V}^{-1} \text{ s}^{-1}$), large current on/off ratios ($I_{\text{on}}/I_{\text{off}} > 10^6$), and low threshold voltages ($< \pm 2.5 \text{ V}$) are still desirable.

Rylene diimides are interesting candidates and many high-mobility examples have been reported.⁷ In particular, materials based on naphthalene-1,8:4,5-bis(dicarboximide)s (NDIs) are among the best organic ET materials to date; some examples show air-stable n-channel mobility values of up to $1.2 \text{ cm}^2 \text{ V}^{-1} \text{ s}^{-1}$ when incorporated in OFETs by vacuum deposition.^{8,9} However, solution-processed ET materials based on NDI derivatives typically exhibit lower mobility values¹⁰ and only recently have values exceeding $\sim 0.1 \text{ cm}^2 \text{ V}^{-1} \text{ s}^{-1}$ been reported. An ET copolymer of NDI and bithiophene reported by Facchetti et al.¹¹ represents the highest mobility example of a solution-processable polymer, with an OFET mobility value of $0.85 \text{ cm}^2 \text{ V}^{-1} \text{ s}^{-1}$. The highest OFET electron mobility values reported to date for solution-cast small molecules have been measured on core-expanded NDIs reported by Zhu et al.,^{12,13} very recently, one of these derivatives was shown to exhibit values as high as $0.55\text{--}1.2 \text{ cm}^2 \text{ V}^{-1} \text{ s}^{-1}$ when appropriately processed,¹³ further demonstrating the potential of rylene-based materials for high-performance solution-processed n-channel OFETs. Here, we report that bis(NDI) derivatives with conjugated bridging groups based on fused heterocycle ring systems can be processed from solution into films that exhibit OFET electron mobility values of up to $1.5 \text{ cm}^2 \text{ V}^{-1} \text{ s}^{-1}$, which is among the highest yet reported for an n-channel OFET based on a solution-processed small molecule.

As shown in Scheme 1, palladium-catalyzed Stille coupling of a brominated NDI, **1**,^{14,15} and distannyl fused-ring heterocycle derivatives, **2**,^{16,17} yields the bis(NDI) derivatives, **NDI2-X** in 30–60% yield; these compounds were characterized by ¹H and

Scheme 1. General Synthesis of NDI2-X

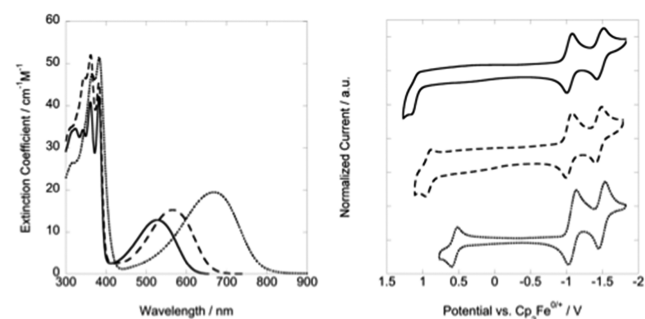
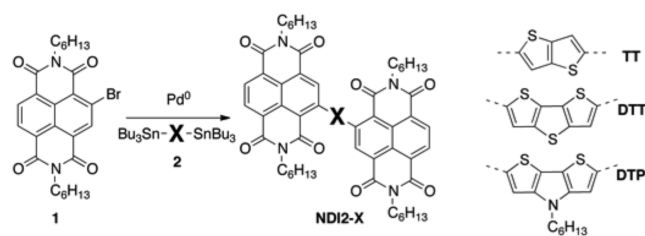


Figure 1. UV–vis absorption in chloroform (left) and cyclic voltammetry (right) of **NDI2-TT** (solid), **NDI2-DTT** (dashed), and **NDI2-DTP** (dotted).

¹³C NMR spectroscopy, high-resolution mass spectrometry, elemental analysis, TGA, and DSC.

The UV–vis absorption spectra (Table 1, Figure 1) of the **NDI2-X** derivatives in chloroform have maxima at 382–385 nm, similar to that of the corresponding monomeric NDI derivative (383 nm). Additionally, **NDI2-TT**, **NDI2-DTT**, and **NDI2-DTP** exhibit long-wavelength absorption maxima at 543, 566, and 681 nm, respectively. The bathochromic shift of this long-wavelength absorption with increasing electron-richness of the bridging group is suggestive of a charge-transfer (CT) type

Received: June 17, 2011

Published: July 18, 2011

Table 1. Optical, Electrochemical,^a Thermal, and Field-Effect Transistor Properties^b of NDI2-X

X	λ_{\max}^c /nm	$\epsilon^c \times 10^{-3}$ /M ⁻¹ cm ⁻¹	$\lambda_{\max, \text{solid}}$ /nm	$E_{1/2}^{+/0}$ /V	$E_{1/2}^{0/2-}$ /V	$E_{1/2}^{2-/-4-}$ /V	T_d^d /°C	μ_e /cm ² V ⁻¹ s ⁻¹	V_{TH} /V	$I_{\text{on}}/I_{\text{off}}$
TT	383	41.7	335	1.10	-1.05	-1.48	400	0.12 ± 0.02	12.3 (±0.7)	1 × 10 ⁴
	543	12.8	572							
DTT	382	40.5	362	0.93	-1.03	-1.45	402	0.14 (±0.07)	9.0 (±0.3)	2 × 10 ³
	566	14.8	570							
DTP	385	52.9	400	0.56	-1.09	-1.50	409	1.2 (±0.3)	13.0 (±0.9)	^e
	681	19.9	744							

^a In CH₂Cl₂/0.1 M ⁿBu₄NPF₆ vs FeCp₂^{+/0}. ^b Average n-channel saturation-region field-effect mobility (μ_e), threshold voltage (V_{TH}), and current on/off ratio ($I_{\text{on}}/I_{\text{off}}$) for top-gate bottom-contact OFETs based on solution-processed NDI2-X layers. ^c In CHCl₃. ^d Defined as temperature at which a 5% mass loss is seen by TGA. ^e Not determined because of ambipolarity of sample.

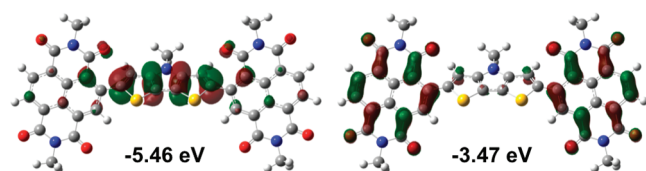


Figure 2. Pictorial representation of the HOMO (left) and LUMO (right) wavefunctions for NDI2-DTP as determined at the B3LYP/6-31G** level of theory.

origin. Moreover, the low-energy band is similar to that seen in other thiophene-substituted NDIs.¹¹

Density functional theory (DFT) calculations at the B3LYP/6-31G** level were used to investigate the (gas-phase) neutral ground state, while time-dependent DFT (TDDFT) calculations were used to examine the $S_0 \rightarrow S_n$ vertical ground-to-excited-state transitions. The TDDFT results, using either the B3LYP or long-range-corrected CAM-B3LYP and ω B97X functionals, reveal that indeed the low-lying transitions have charge-transfer-like character.¹⁸ In general, absorption profiles for the visible region generated with the three density functionals are in good agreement. The B3LYP $S_0 \rightarrow S_1$ transition energies were calculated to be 1.95, 1.84, and 1.70 eV (636, 674, and 729 nm) for NDI2-TT, NDI2-DTT, and NDI2-DTP, respectively, with the transitions dominated by electronic excitation from the HOMO \rightarrow LUMO (98, 88, and 85%, respectively). HOMO and LUMO single-electron wavefunction distributions (B3LYP/6-31G**) are depicted in Figure 2 and Figures S2 and S3 of the Supporting Information. The HOMO wavefunctions are localized on the central electron-rich units for all three NDI2-X derivatives. The LUMOs are almost entirely localized on the two NDI segments and their energies are within 0.13 eV of that of an isolated NDI.

Cyclic voltammetry (CV) was used to measure the electrochemical properties of the NDI2-X derivatives in CH₂Cl₂/0.1 M ⁿBu₄NPF₆ (Table 1, Figure 1). In each case, a one-electron reversible oxidation process was observed along with two reversible reduction processes, each with approximately twice the current of that found for the oxidation; these are assigned to essentially independent reduction of both NDIs to their radical anions to give a molecular dianion and then a second reduction of both NDIs to give a tetraanion (Table 1, Figure 1). The first half-wave reduction ($E_{1/2}^{0/2-}$) potentials are very similar to that of an isolated NDI core ($E_{1/2}^{0/2-} = -1.34$ V), consistent with the similarity in the DFT LUMO energies of the NDI2-X compounds and isolated NDIs noted above. The half-wave oxidation ($E_{1/2}^{+/0}$) potentials show a difference between the

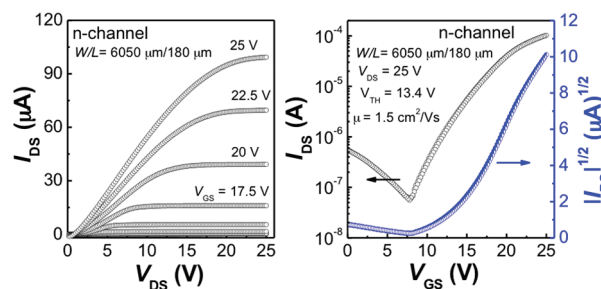


Figure 3. Output (left), and transfer (right) characteristics for n-channel operation of a particular top-gate OFET with NDI2-DTP as semiconductor and CYTOP/Al₂O₃ gate dielectric layer with Au source/drain electrodes ($W/L = 6050 \mu\text{m}/180 \mu\text{m}$).

potentials for DTT and DTP, which reflects that between 2,6-dibutyl-4H-dithieno[3,2-*b*:2',3'-*d*]thiophene and 4-(*tert*-butyl)-2,6-dibutyl-4H-dithieno[3,2-*b*:2',3'-*d*]pyrrole ($E_{1/2}^{+/0} = 0.69$ and 0.23 V, respectively),¹⁹ consistent with DFT data showing the HOMOs to be largely localized on the bridging groups; DFT adiabatic ionization potentials also show similar trends (6.83, 6.65, and 6.35 eV in NDI2-TT, NDI2-DTT and NDI2-DTP, respectively).

Electrical characterization studies (Table 1) were performed on top-gate OFETs with a CYTOP/Al₂O₃ bilayer gate dielectric²⁰ and Au source/drain electrodes (Supporting Information). NDI2-X was spin-coated from 1,2-dichlorobenzene solutions; however, uniform films were not obtained from spin-casting of NDI2-TT and NDI2-DTT due to reduced solubility of these materials in dichlorobenzene, and so films of these materials were prepared by drop casting.

OFETs fabricated using NDI2-DTP showed ambipolar electrical characteristics with dominant n-channel transistor behavior. Devices exhibited electron mobility values of up to 1.5 cm² V⁻¹ s⁻¹ with a rather high threshold voltage of 13.0 V (Figure 3). In p-channel transistor operation (Figure S10 of the Supporting Information), a hole mobility of up to 9.8 × 10⁻³ cm² V⁻¹ s⁻¹ with a threshold voltage of -14.4 V was observed. The ambipolarity of NDI2-DTP means that the transistors are not fully turned off at zero gate bias and that no $I_{\text{on}}/I_{\text{off}}$ can be measured, which is problematic for applications. On the other hand, decreasing the donor character of the bridge led to purely n-channel device performance and moderate on/off ratios; devices based on NDI2-TT and NDI2-DTT function solely as n-channel transistors, albeit with lower mobility values than that seen for NDI2-DTP and with comparably high threshold voltages. Studies are underway to further

optimize the properties and device characteristics of this class of materials.

■ ASSOCIATED CONTENT

S Supporting Information. Full synthesis and characterization of NDI2-X, including OFET device fabrication and characterization details. This material is available free of charge via the Internet at <http://pubs.acs.org>.

■ AUTHOR INFORMATION

Corresponding Author

*E-mail: seth.marder@gatech.edu (S.R.M.), kippelen@ece.gatech.edu (B.K.).

Present Address

^{||}Current address: Indian Institute of Technology Rajasthan, Jodhpur, Rajasthan, 342011, India.

■ ACKNOWLEDGMENT

This research was financially supported by Solvay S.A. and through the STC Program of the National Science Foundation (DMR 0120967). The authors gratefully acknowledge Tissa Sajoto for the synthesis of an intermediate and Jungbae Kim and Keith Knauer for their help with the metal deposition during OFET device fabrication.

■ REFERENCES

- (1) Dimitrakopoulos, C. D.; Malenfant, P. R. L. *Adv. Mater.* **2002**, *14*, 99.
- (2) Sirringhaus, H.; Ando, M. *MRS Bull.* **2008**, *33*, 676.
- (3) Garnier, F.; Hajlaoui, R.; Yassar, A.; Srivastava, P. *Science* **1994**, *265*, 1684.
- (4) Murphy, A.; Fréchet, J. *Chem. Rev.* **2007**, *107*, 1066.
- (5) Anthony, J. E.; Facchetti, A.; Heeney, M.; Marder, S. R.; Zhan, X. *Adv. Mater.* **2010**, *22*, 3876.
- (6) Dong, H.; Wang, C.; Hu, W. *Chem. Commun.* **2010**, *46*, 5211.
- (7) Zhan, X.; Facchetti, A.; Barlow, S.; Marks, T. J.; Ratner, M. A.; Wasielewski, M. R.; Marder, S. R. *Adv. Mater.* **2010**, *23*, 268.
- (8) Shukla, D.; Nelson, S. F.; Freeman, D. C.; Rajeswaran, M.; Ahearn, W. G.; Meyer, D. M.; Carey, J. T. *Chem. Mater.* **2008**, *20*, 7486.
- (9) See, K. C.; Landis, C.; Sarjeant, A.; Katz, H. E. *Chem. Mater.* **2008**, *20*, 3609.
- (10) Katz, H. E.; Lovinger, A. J.; Johnson, J.; Kloc, C.; Siegrist, T.; Li, W.; Dodabalapur, Y.-Y. L. A. *Nature* **2000**, *404*, 478.
- (11) Yan, H.; Chen, Z.; Zheng, Y.; Newman, C.; Quinn, J. R.; Dötz, F.; Kastler, M.; Facchetti, A. *Nature* **2009**, *457*, 679.
- (12) Gao, X.; Di, C.-A.; Hu, Y.; Yang, X.; Fan, H.; Zhang, F.; Liu, Y.; Li, H.; Zhu, D. *J. Am. Chem. Soc.* **2010**, *132*, 3697.
- (13) Zhao, Y.; Di, C.; Gao, X.; Hu, Y.; Guo, Y.; Zhang, L.; Liu, Y.; Wang, J.; Hu, W.; Zhu, D. *Adv. Mater.* **2011**, *23*, 2488.
- (14) Chaignon, F.; Falkenstrom, M.; Karlsson, S.; Blart, E.; Odobel, F.; Hammarstrom, L. *Chem. Commun.* **2007**, 64.
- (15) Jones, B. A.; Facchetti, A.; Marks, T. J.; Wasielewski, M. R. *Chem. Mater.* **2007**, *19*, 2703.
- (16) Zhan, X.; Tan, Z.; Domercq, B.; An, Z.; Zhang, X.; Barlow, S.; Li, Y.; Zhu, D.; Kippelen, B.; Marder, S. R. *J. Am. Chem. Soc.* **2007**, *129*, 7246.
- (17) Zhang, X.; Steckler, T.; Dasari, R.; Ohira, S.; Potscavage, W. J.; Tiwari, S. P.; Coppée, S.; Ellinger, S.; Barlow, S.; Brédas, J.-L.; Kippelen, B.; Reynolds, J. R.; Marder, S. R. *J. Mater. Chem.* **2010**, *20*, 123.
- (18) While the TDDFT vertical transition energies to the first excited states determined with the B3LYP functional are red-shifted

with respect to the experiment, those determined with both the CAM-B3LYP and ω B97X functionals are blue-shifted; see Supporting Information for further details.

(19) Barlow, S.; Odom, S. A.; Lancaster, K.; Getmanenko, Y. A.; Mason, R.; Coropceanu, V.; Brédas, J.-L.; Marder, S. R. *J. Phys. Chem. B* **2010**, *114*, 14397.

(20) Hwang, D. K.; Fuentes-Hernandez, C.; Kim, J.; Potscavage, W. J.; Kim, S.-J.; Kippelen, B. *Adv. Mater.* **2011**, *23*, 1293.